Available online at www.sciencedirect.com
ScienceDirect
Journal of Solid State Chemistry 179 (2006) 2875–2879
JOURNAL OF SOLID STATE CHEMISTRY
www.elsevier.com/locate/jssc

The morphology of ceramic phases in B_xC–SiC–Si infiltrated composites

S. Hayun, N. Frage*, M.P. Dariel

Department of Materials Engineering, Ben-Gurion University of the Negev, P.O. Box 653, Beer-Sheva 84105, Israel

Received 1 September 2005; received in revised form 20 October 2005; accepted 16 January 2006
Available online 17 February 2006

Abstract

The present communication is concerned with the effect of the carbon source on the morphology of reaction bonded boron carbide (B_4C). Molten silicon reacts strongly and rapidly with free carbon to form large, faceted, regular polygon-shaped SiC particles, usually embedded in residual silicon pools. In the absence of free carbon, the formation of SiC relies on carbon that originates from within the boron carbide particles. Examination of the reaction bonded boron carbide revealed a core–rim microstructure consisting of boron carbide particles surrounded by secondary boron carbide containing some dissolved silicon. This microstructure is generated as the outcome of a dissolution–precipitation process. In the course of the infiltration process molten Si dissolves some boron carbide until its saturation with B and C. Subsequently, precipitation of secondary boron carbide enriched with boron and silicon takes place. In parallel, elongated, strongly twinned, faceted SiC particles are generated by rapid growth along preferred crystallographic directions. This sequence of events is supported by X-ray diffraction and microcompositional analysis and well accounted for by the thermodynamic analysis of the ternary B–C–Si system.

Keywords: Boron carbide; Reaction bonding; SiC; Core–rim structure

1. Introduction

Reaction bonded silicon carbide (RBSC) refers to a group of composites processed by infiltrating with molten silicon a green compact or a partially sintered mixture of SiC particles and carbon, in order to obtain a fully dense composite. The molten silicon reacts with free carbon and secondary SiC is formed. The newly formed silicon carbide particles and the 5–15 vol% residual silicon bond the pre-existing SiC particles into a cohesive and hard solid [1]. A detailed study of SiC formation by the reaction bonding process [2] revealed that silicon carbide always grows as the β-polytype and usually nucleates onto existing SiC particles. Secondary β-SiC may also nucleate on carbon or even homogeneously within the liquid Si.

The addition of boron carbide, B_4C, to the initial SiC–carbon mixture leads to improved mechanical properties of the composite and, in fact, boron carbide may be reaction bonded in a way similar to RBSC. Reaction bonded boron carbide is denoted RBBC. Moreover, boron carbide may act as an alternative source of carbon for the formation of secondary SiC [3]. Two potential carbon sources are consequently present, namely, free carbon in the mixture and/or carbon originally present in the carbide phase. It is reasonable to assume that the actual source of carbon affects the morphology of the growing SiC particles and thereby the mechanical properties of the RBBC composite.

In the present study, the evolution of the ceramic phases morphology in RBBC as a function of the carbon source is described. Two methods of the composite preparation were investigated: partially sintered boron carbide preforms or partially sintered boron carbide preforms saturated with free carbon were infiltrated with silicon, yielding composites, denoted *type-A* and *type-B*, respectively.

2. Experimental procedure

2.1. Fabrication of type-A and type-B composites

Compacts, 20 mm in diameter and 3 mm high, were manufactured from boron carbide powder (~5 μm) by

*Corresponding author. Fax: +972 8 647941.
E-mail address: nfrage@bgu.ac.il (N. Frage).

0022-4596/$ - see front matter © 2006 Elsevier Inc. All rights reserved.
doi:10.1016/j.jssc.2006.01.031

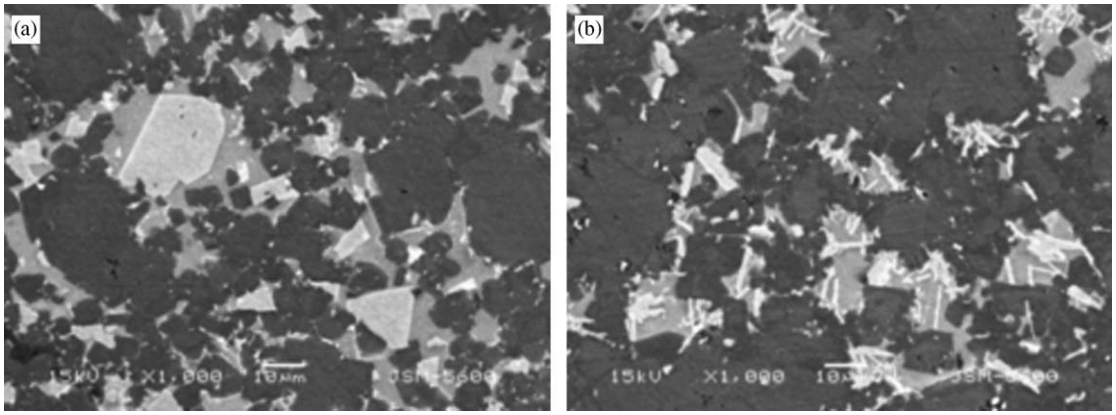

Fig. 1. Microstructure (SEM image) of the composites prepared without (type-A(b)) and with free carbon additions (type-B(a)). The initial open porosity of the preforms was about 20 vol%.

uniaxial compaction (25 MPa). The powder was supplied by "Modan Jang", a Chinese Company. The composition of the powder has been reported in our previous paper [4]. The compacts were sintered in the 2173–2373 K temperature range for 30 min, and preforms with 20–40 vol% porosity were obtained. For the fabrication of the type-B composites, free carbon was added to the porous preforms by infiltration with an aqueous sugar solution (50:50). The infiltrated preforms were dried and heat treated at 773 K in order to pyrolize the sugar. The preforms with and without free carbon were infiltrated with Si in a vacuum furnace (10^{-4} torr). Infiltration was carried out by placing an appropriate amount of Si lump on top of the porous preforms and heating to 1723 K for 20 min.

2.2. Microstructural investigation

The microstructure of the samples was studied using optical microscopy (OM, Zeiss Axiovert 25), scanning electron microscopy (SEM, JEOL-35) in conjunction with an energy-dispersive spectrometer (EDS) and wavelength-dispersive spectrometer (WDS) and a transmission electron microscope (TEM, JEOL-2010). The samples for the OM and SEM characterization were prepared using a standard metallographic procedure that included a last stage of polishing by 1 μm diamond paste. Image analysis was performed using the Thixomet[1] software in order to determine the amount of residual Si in the composites.

The samples for TEM characterization were prepared as follows: 1 mm thick foils were cut using 0.4 mm diamond saw and ground down to 500 μm. Disks of 3 mm diameter were drilled with cooper drill pipe and 40 μm diamond paste, ground down to 70 μm thickness, and polished to 30 μm thickness. The perforation stage was carried out using a Gatan™-precision ion polishing system.

[1]Image analysis program, developed at the St. Petersburg State Polytechnic University, Department of Steel and Alloys.

3. Results and discussion

3.1. Microstructural analysis

The microstructures of the *type-B* and *type-A* composites are shown in Figs. 1a and b. In the *type-A* composites, the SiC phase appears as white plate-like particles (Fig. 1b). These particles are always adjacent to the boron carbide grains. The SiC phase in the *type-B* composites displays an irregular polygonal form and only a small fraction of the particles has the plate-like form. The light-gray regions correspond to residual Si, and the dark gray areas correspond to the partially sintered boron carbide skeleton. According to the image analysis of the microstructure (Table 1), the relative amounts of the SiC phase are similar for the composites prepared with and without free carbon addition for a certain initial porosity of the preforms. The amount of the SiC phase slightly increased from 8 to 12 vol% with an increase of the initial porosity of the preforms from 20 to 40 vol%.

The analysis of the microstructures provides a clue to the mechanism of the SiC phase formation in the *type-A* and *type-B* composites. In *type-B* composites, after dissolution of the free carbon in the melt, the SiC phase precipitates on the melt/graphite interface.

A similar mechanism has been put forward for reaction bonded SiC–Si composites [2]. After consumption of the free carbon, liquid silicon continues to react with boron carbide and some additional plate-like particles, attached to the boron carbide grains, are formed.

In the *type-A* samples, liquid silicon directly reacts with boron carbide and the evolution of the microstructure appears to be more complex. Careful examination of the *type-A* microstructure reveals a "core–rim" structure of the boron carbide phase. A similar structure had been described by Ahn and Kang [5,6] in conjunction with the microstructure of various transition metal carbide phases. This "core–rim" structure consists of an inner boron carbide core surrounded by a 3–7 μm thick envelope. The contrast between the core and the envelope is weak and in

Table 1
Average phase distribution in type-A and type-B composites

Materials	Carbon addition (vol%)	Boron carbide (vol%)	Silicon (vol%)	Silicon carbide (vol%)
Type-A	0	80±3	12±1	8±1
	0	70±3	20±1	10±1
	0	60±3	28±1	12±1
Type-B	3±0.5	80±3	12±1	8±1
	4±0.5	70±3	21±1	9±1
	6±0.5	60±3	30±1	10±1

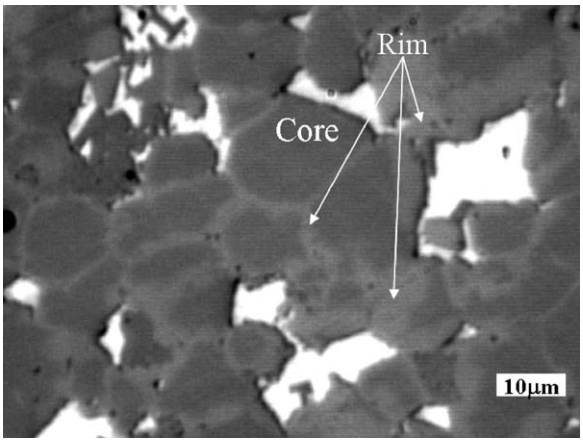

Fig. 2. Optical image of the core–rim structure of the boron carbide phase.

some instances it is difficult to distinguish between the two regions, as shown in Fig. 2.

A WDS line-scan across the envelope and the core is shown in Figs. 3a and b and reveals the presence of Si within the rim region. The distance (3–7 μm) over which the Si compositional change takes place corresponds to the width of the rim, as revealed by its contrast with the core. One reason for the presence of a Si compositional profile within the rim may be due to silicon diffusion into the carbide phase. The possibility of silicon dissolution in boron carbide at a significantly higher temperature (2220 K) was reported in [7,8]. The width of this compositional profile is not consistent however with known values of the diffusivities within boron carbide at temperatures corresponding to the infiltration step of the process [9]. It should be noted also that boron carbide within the rim region has a higher B/C ratio than that within the core region (Fig. 3a).

3.2. X-ray diffraction

The assumption of two distinct boron carbide phases is further supported by the results of XRD analysis. The XRD patterns (Fig. 4) of the *type-A* composite revealed two clearly distinct boron carbide patterns with different lattice parameters. One of these phases is the original boron carbide with a boron to carbon ratio of 4:1 and lattice parameters, $a = 0.55592 \pm 0.0002$ nm and $c = 1.2052 \pm 0.0010$ nm. The second boron carbide phase has a distinctly larger lattice parameter, $a = 0.55637 \pm 0.0005$ nm and $c = 1.2338 \pm 0.0015$ nm.

A higher boron to carbon ratio has been reported to increase the a and c lattice parameters of boron carbide [10]. This increase, however, is not commensurate with the measured lattice parameters. The significantly larger increase in particular of the c lattice parameter is to be attributed to the presence of silicon dissolved in the boron carbide lattice [7].

3.3. Dissolution–precipitation process

An alternative explanation for the formation of the core–rim microstructure is a dissolution–precipitation mechanism that became operative in the course of the infiltration. This mechanism is based on the fact that the concentration of the surrounding dissolved elements is higher in the vicinity of the below average size boron carbide particles on account of their higher chemical potential. A chemical gradient is set up that causes a flux of B, C in the molten medium from the small to the large particles. The precipitation of B_xSi_yC layers on the relatively coarse boron carbide particles takes place. The dissolution–precipitation mechanism may be considered using an isothermal section of the ternary Si–B–C diagram. The constructed schematically isothermal section for a temperature above the melting point of Si (Fig. 5) is based on the investigations of Telle [7] and Seifert and Aldinger [11].

Above the melting point of Si, a single-phase domain, Si_L, delineated by the limits of solubility of B and of C in molten Si, lies at the upper corner of the phase diagram. A two-phase B_xC and Si_L region is also established in which the compositions of the phases coexisting in equilibrium are linked by tie-lines. The initial B_4C–Si mixtures of various compositions have to be located on the dashed line 1. Actually, for the systems with Si excess (infiltrating conditions), an initial total composition corresponds to point 1 and is located within the two-phase region. Since the total composition of the system does not change during interaction (point 1 remains at the same position) it leads to carbide decomposition and the formation of Si–B–C liquid solution, which is in equilibrium with boron carbide enriched with B. SiC is not stable at this stage of the interaction. Precipitation of Si-containing and B-enriched boron carbide takes place on the relatively coarse ceramic particles and leads to a decreasing amount of Si in the melt. The composition of the system in the vicinity of the carbide particles shifts to point 2 and enters the three-phase domain in which the SiC phase is stable and makes its apparition. The system, evidently, is very close to the boundary between the two- and three-phase regions. In this case, C and Si concentration gradients are relatively small and promote the plate-like SiC formation. A rapid increase

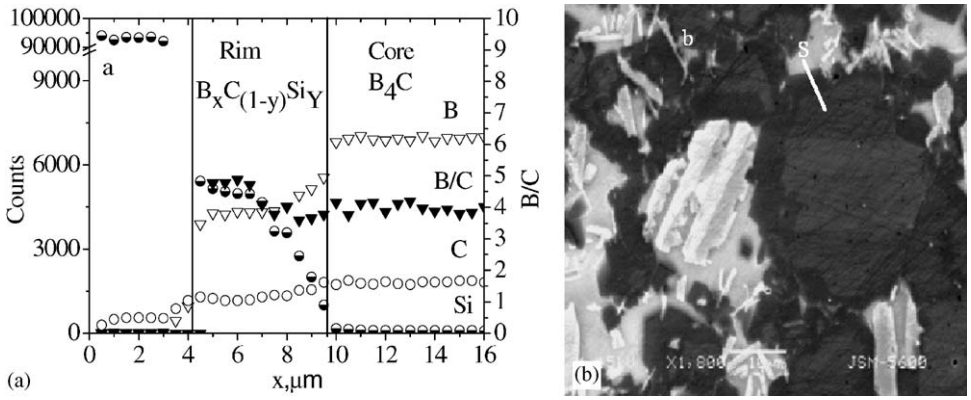

Fig. 3. Line-scan (a) along the straight white line in the secondary electron image (b) of *type-A* composite.

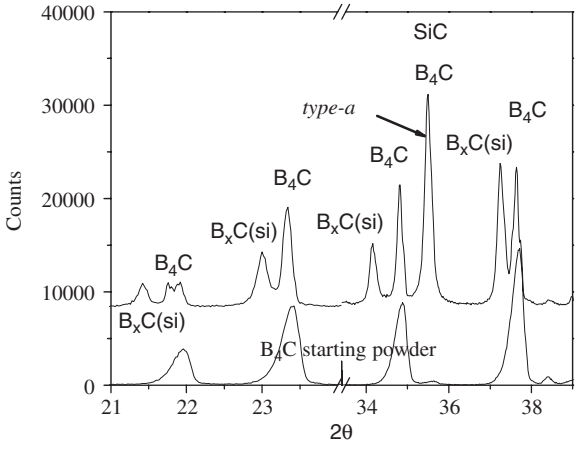

Fig. 4. XRD patterns of B_4C and *type-A* composite. In the X-ray spectrum all the diffraction lines corresponding to the boron carbide phase appear as doublets indicating the presence of two different phases differing in their composition.

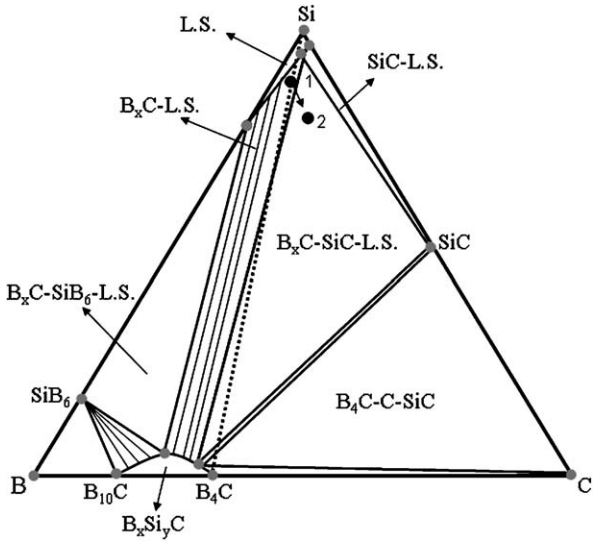

Fig. 5. Isothermal section of the ternary B–C–Si system at a temperature above the melting point of Si.

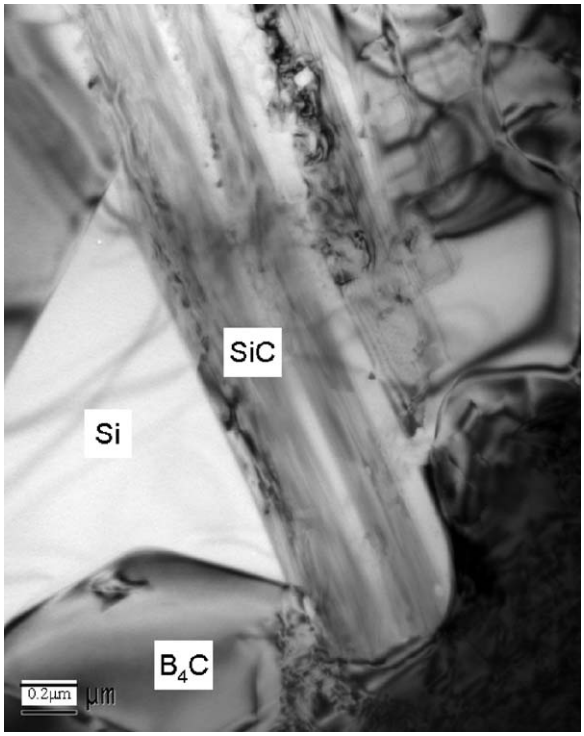

Fig. 6. TEM bright field image of type-A composite.

of observed thickness of the envelope is due to rapid mass transport within the liquid.

3.4. TEM analysis

To further enhance our understanding of the microstructure of the plate-like β-SiC, a cursory TEM analysis was carried out. A bright field image of a *type-A* sample is shown in Fig. 6 with three phases, boron carbide, silicon carbide and residual silicon in close contact. The β-SiC grain consists of a stack of twins as shown in Fig. 7.

A bright field image of the intermediate area between two adjacent boron carbide grains is shown in Fig. 8. This area is heavily faulted and can be identified with the envelope surrounding the initial boron carbide grains. It

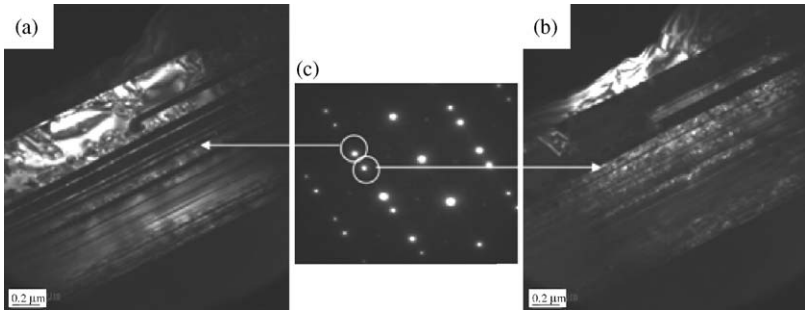

Fig. 7. Dark field images of the twins in the β-SiC grain (a and b). Notice that the two twins complement each other. Selected area diffraction of the two twins (c).

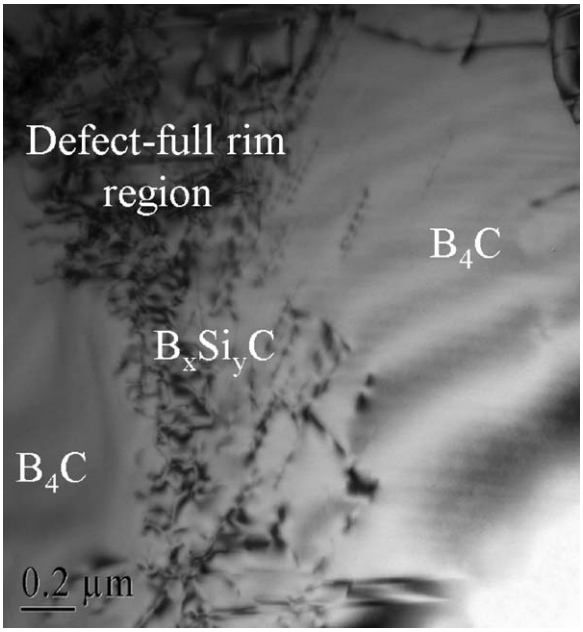

Fig. 8. Bright field TEM image of the rim area between two boron carbide grains.

corresponds to the secondary boron carbide formed by precipitation from the molten silicon solution. According to EDS examination, it contains approximately 2 wt% Si dissolved in the boron carbide matrix, which is consistent with the X-ray diffraction results.

Thus, the dissolution–precipitation mechanism is an essential feature of the reaction bonding process in RBBC. It depends on the solubility of B and C in liquid Si. Moreover, it must be considered that it is a process which critically depends on the local conditions prevailing in each microregion. In such regions, the amount of molten Si varies during the infiltration process and so do the amounts of C and of B dissolved in the molten matrix. This in turn affects the precipitation process, the formation of the secondary Si-containing boron carbide that cements the pre-existing boron carbide particles into the cohesive and hard composite.

4. Conclusions

Reaction bonding of boron carbide by molten silicon infiltration is possible even in the absence of an external carbon source. The microstructure evolution of such RBBC in the absence of external carbon could be attributed to a dissolution–precipitation process. In the course of the infiltration, molten silicon saturates with boron and carbon. Secondary boron carbide, containing some Si in solid solution, precipitates on the relatively coarse initial boron carbide particles and forms a core–rim structure generating the cohesive solid.

The formation of the rim–core structure and the plate-like SiC phase is well accounted for by the analysis of the isothermal section of the B–C–Si ternary system.

Acknowledgments

We wish to thank Dr. L. Dilman for her assistance in sample preparation, Mr. M. Aizenstein for some WDS analysis and Mr. V. Ezersky for the TEM analysis.

References

[1] Y.M. Choing, R.P. Messner, C.D. Terwilliger, D.R. Behrendt, Mater. Sci. Eng. A 144 (1991) 63–74.
[2] J.N. Ness, T.F. Page, J. Mater. Sci. 21 (1986) 1377–1397.
[3] I.S. Han, K.S. Lee, D.W. Seo, S.K. Woo, J. Mater. Sci. Lett. 21 (2002) 703–706.
[4] N. Farge, L. Levin, M.P. Dariel, J. Solid State Chem. 177 (2004) 410–414.
[5] S. Ahn, S. Kang, Int. J. Refract. Metals Hard Mater. 19 (2001) 539–545.
[6] S. Ahn, S. Kang, J. Am. Ceram. Soc. 83 (6) (2000) 1489–1494.
[7] R. Telle, in: R. Freer (Ed.), The Physics and Chemistry of Carbides, Nitrides and Borides, Kluwer Academic Publishers, Dordrecht, 1990, p. 249.
[8] R. Telle, G. Petzow, in: P. Vincenzini (Ed.), High Tech Ceramics C, Elsevier Publisher, Amsterdam, 1987, pp. 961–973.
[9] T. Hase, H. Suzuki, Communication of the American Ceramic Society, 1981 (Chapter 58).
[10] F. Thévenot, J. Eur. Ceram. Soc. 6 (1990) 205–225.
[11] H.J. Seifert, F. Aldinger, Struct. Bonding 101 (2002) 1–58.